



Journal of Mining and Environment (JME)

journal homepage: [www.jme.shahroodut.ac.ir](http://www.jme.shahroodut.ac.ir)



## Facies Quality Zoning in Shale Gas by Deep Learning Method

Yousef Asgari Nezhad, and Ali Moradzadeh\*

School of Mining Engineering, College of Engineering, University of Tehran, Tehran, Iran

### Article Info

Received 13 December 2020  
Received in Revised form 15  
January 2021  
Accepted 20 January 2021  
Published online 20 January 2021

DOI:10.22044/jme.2021.10366.1983

### Keywords

Facies quality zoning  
Deep learning  
Petro-physical logs  
Seismic  
Canning basin

### Abstract

One of the most essential factors involved in unconventional gas reserves for drilling and production is a suitable quality facies determination. The direct core and geochemical analyses are the most common methods used for studying this quality. Due to the lack of this data and the high cost, the researchers have recently resorted to the indirect methods that use the common data of the reservoir (including petro-physical logs and seismic data). One of the major problems in using these methods is that the complexities of these reproducible repositories cannot be accurately modeled. In this work, the quality of facies in shale gas is zoned using the deep learning technique. The applied method is long short-term memory (LSTM) neural network. In this scheme, the features required for zoning are automatically extracted and used to model the reservoir complexities properly. The results of this work show that zoning is done with an appropriate accuracy (86%) using the LSTM neural network, while it is 78% for a conventional intelligent MLP network. This specifies the superior accuracy of the deep learning method.

### Nomenclature

CALI: Caliper  
DT: Interval transit time  
GR: Gamma-ray  
LLD: Latrolog deep  
NPHI: Neutron porosity  
RHOB: Bulk density  
SP: Spontaneous potential  
AI: Acoustic impedance  
TOC: Total organic carbon  
 $T_{Max}$ : Maximum of temperature  
BQ: Bad quality  
GQ: Good quality

### 1. Introduction

Unconventional gas resources are important energy resources that have been successfully developed throughout the world in the current century [1, 2]. Many studies have been done on the structural progress, pore features, and existence

mechanisms of shale gas [3-9]; however, the quantitative characterization of shale gas quality is relatively rare. At the present time, some experiments such as the geochemical, routine test, and X-ray diffraction are used in order to check some shale properties [10]. Also in gas-rich reservoirs, the response of surface geophysics (seismic) and well-log interpretation is very practical [11].

The facies quality has been usually applied to petro-physical logs. Sandstone and limestone are defined based on GR log and neutron-density cross plot. Lower Cambrian shales in Cengong block are associated with the high GR and total organic carbon (TOC) values. The low amounts of thorium (Th) and potassium (K) suggest a low clay content. Neutron-density cross-over is generally linked with the gas-bearing shale beds [12]. Brittle shale beds have been well-developed, and the gas storage capacity of the lower Cambrian shale reservoir has been affected by faulting and folding, to some extent [13]. Some researchers have used petro-

Corresponding author: [a\\_moradzadeh@ut.ac.ir](mailto:a_moradzadeh@ut.ac.ir) (A. Moradzadeh).

physical logs in order to model the geochemical parameters of reservoirs such as TOC or maturity of gas or oil in gas shales [14-20].

The geophysical responses have been used in modelling and characterization of the facies quality. For example, a quantitative study has been done about the effect of TOC on the seismic elastic parameters by a measurement of the artificial rock samples under specific formation pressures. [21]. Ashraf *et al.* (2019) have evaluated the sand facies with combination of electro-facies analyses, historical production data, and seismic attribute analyses. Also in order to achieve the maximum production, they used 3D seismic and well log data [22]. Some researchers have used this idea to acquire a high efficiency and realize an actual production of shale gas [23-25]. Daniel *et al.* (2009) have found out that the gas content has a good relation with porosity and TOC [26].

According to what mentioned above, various qualitative and quantitative approaches have been applied to determine the quality of gas-containing facies. In a qualitative modeling, the various characteristics of the formations must be accurately obtained. Rock facies of formations are considered as an important parameter in identifying the heterogeneity in each layer. In the quantitative method, the quality of gas and oil facies is determined by the quantitative data using the thresholds related to the desired organic matter. The most common data used in a direct quantitative estimation method is the geochemical data. The biggest problem is the lack of this data due to its cost, and this causes the accuracy of the models and their evaluations to be affected. Hence, many researchers have turned to the indirect evaluations. Due to the complexity of the relationships between the geochemical and geophysical parameters, the methods based on simple or multivariate regression fitting have given way to the intelligent methods. In this work, it was attempted to use a new direct quantitative method. This complex model is deep learning (LSTM neural network), which uses the seismic and petro-physical data for zoning the quality of gas facies.

## 2. Studied area and dataset

The Canning basin is a large complex basin with a NW-SE trend, which is located in northwestern Australia [27-29]. This is a completely coastal sedimentary basin with an area of about 595,000 square kilometers. Its northwestern trend is controlled by the Precambrian cratons that surround the Canning basin [28].

Sediments of Ordovician age, in fault-controlled sub-basins, have started with the coarse silicate marginal sediments and shallow marine sediments of the Nambit formation. An increased marine progress leads to sedimentation of the Willara formation in most of the Canning basin covered by carbonate of the Nambite formation [30]. The maximum inundation is characterized by the widespread deposition of Goldwyer formation in Ordovician including the bromine platform with the greatest distance from the center below the Kidston and Willara basins [31]. This formation mainly consists of shales with nested limestone rocks that are located in confined marine environments and also includes graptolites, trilobites, brachiopods, condontents, and grappropods [30]. As mentioned earlier, the Goldwyer formation has an excellent potential for organic matter in the areas where many fossil green algae are found [32]. The stratigraphy and petroleum systems of the onshore Canning basin is illustrated in Figure 1.

In this research work, the quality facies zoning was carried out using the petro-physical logs including GR, DT, CALI, SP, RHOB, NPFI, and LLD of a well in a seismic profile and the acoustic impedance (AI) data was acquired by inversion of the post-stack seismic data in the Western Australia. This work focuses on the Goldwyer formation. The geochemical evaluation of the Goldwyer formation is performed from the results listed in the Foster's paper in 1986 [34]. The facies quality in shale gas (for validation of the model as real data) was determined using the organic geochemical data, which was mainly the TOC, maturity, and core reports.

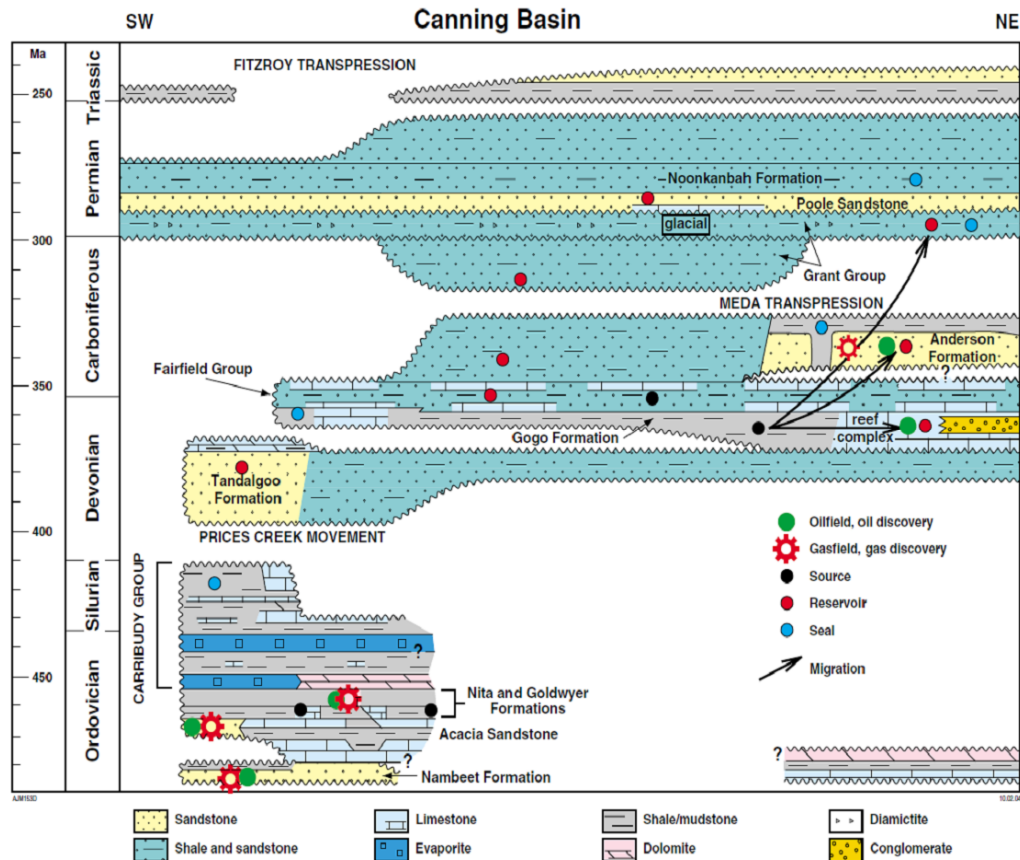


Figure 1. A litho-stratigraphical diagram of petroleum structures for the Canning basin [33].

### 3. Methodology

Machine learning is a sub-division of artificial intelligence, and includes the techniques that enable the computer to recognize the data on its own in order to figure things out and provide the artificial intelligence applications. The reason for why the early researchers found some problems much more difficult was that the problems could not be solved with the basic techniques used in artificial intelligence. Deep learning is a type of machine learning systems that are based on the artificial neural networks (e.g. LSTM that has three types of input, output, and hidden layers) and can be used for unsupervised activities. This is significant in practice as the unlabeled data is more than the labeled data [35, 36]. In this system, every level learns to turn the input data into a somewhat more abstract and hybrid display. What matters is that a deep learning method, on its own, can learn which features to optimally place at which level.

The most recent deep learning models are based on the artificial neural networks. LSTM is a type of the neural networks that is used as a deep learning technique. The LSTM network, like all the neural networks, has three types of input, output, and

hidden layers. LSTM is also one sort of model or structure for serial data that appears for the growth of the recurrent neural networks (RNNs). The LSTM networks have a sequence or chain-like; nevertheless, the iterative unit has a diverse structure. Instead of one layer of the neural networks in the hidden layer, they have four layers in each hidden layer that interact with each other according to a special structure [37].

The first data enters the hidden layer, and the training process in the first layer is done according to the structure shown in Figure 2.

The cell state is actually a conveyor belt that transfers the existing knowledge linearly from one layer to another. The multiplication sign (the result is between zero and one) is to preserve the knowledge or not, and the plural sign means to add a new knowledge. However, what data and how it enters the cell state is determined by the gateways.

The gates generate the data between zero and one with a sigmoid function. Therefore, by performing the multiplication operation in the sigmoid, the share of each data in the transfer and the next steps can be determined. In the first gate from the left, which is called the input gate (forgetting), the new

data is entered, and by specifying a value between zero and one and the multiplication operator, the result obtained is sent to the cell state. The second gate on the left is called the update gate. The new data enters this gate and passes through the sigmoid function like the previous gate; however, before reaching the cell state, it combines with the data of the previous layer, which passes through the transfer function (hyperbolic tangent) and multiplies by the cell state that goes to add to the cell state (with the addition of operator). In fact, the transfer function generates a new knowledge, and the update gateway determines the share of this knowledge to be transferred to the cell state.

Next, in order to construct the network output, the cell state value passes through a hyperbolic tangent operator to set a range of numbers in the

new cell state between -1 and 1. Also in the third gate (output gate), the data required for modeling at the desired depth is selected and the share of each is determined by the sigmoid function. Finally, the output of this gate is multiplied by the output of the cell state, which passes through the hyperbolic tangent operator, and the results are presented as the output of the desired hidden layer. If this hidden layer is not the last hidden layer in the network, this output is sent to the next hidden layer, and this process is repeated in the new hidden layer with the new data. If this hidden layer is the last hidden layer in the network, its output is taken to the output layer. The model's output is matched with the actual data, and the error is obtained. In order to reduce the error, the weights acting on the gates are optimized to minimize the error [38].

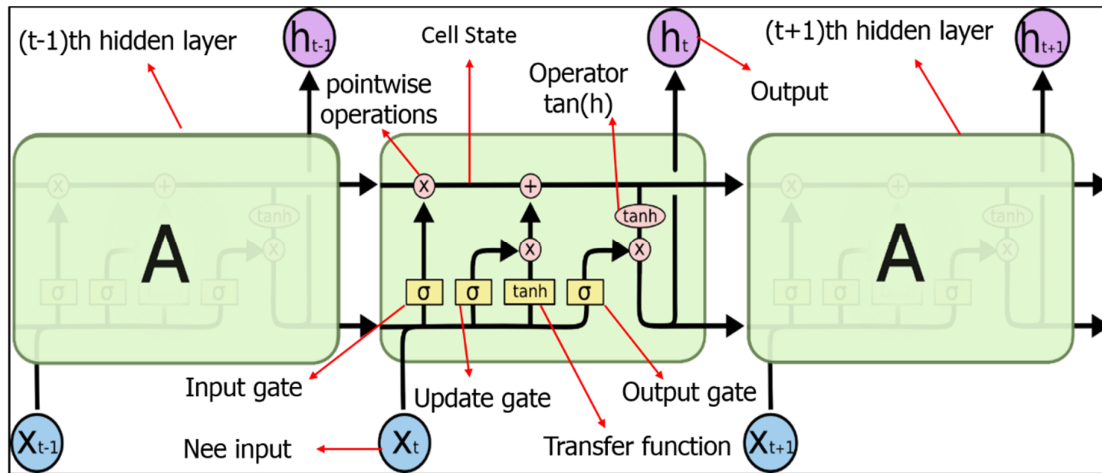


Figure 2. Three hidden layers in an LSTM. The iterating unit in a LSTM comprises four interacting layers (gates and transfer function) in the hidden layers [37].

#### 4. Result and Discussion

For zoning the quality of gas facies, the data is first prepared to enter the network. As stated in Section 2, the data is of two categories. The first category is the petrophysical logs. The second set of data is the post-stack seismic trace, which is inverted using a model-based method to produce the acoustic impedance (AI) data. Then both of them should be normalized using Equation 1.

$$X_{norm} = \frac{x_i - x_{min}}{x_{max} - x_{min}} \quad (1)$$

Here, a two-dimensional (2D) section of the AI data (Figure 3) of a seismic profile is used. Once preparing the data, the quality zoning of gas facies is done using the LSTM network in the interested zone (1270 m-2120 m). Here, the common functions such as the sigmoid (for the input, update, and output gates) and the hyperbolic

tangent (for transfer from the gate to the cell state) are used. By repeating and running the program for several times, it was found that in the best case, the size of the hidden layer was set to 10 with a maximum of 50 epochs. The network specifications used are shown in Table 1. The input data is the petrophysical logs and acoustic impedance. The network first selects the optimal number of zones and then divides the data into these zones and presents the result as a specific code. One of the advantages of this method is that it automatically selects the optimal number of zones. Its mechanism is that the number of optimal zones is the value that has the least error and the highest network efficiency. The results of this zoning are validated by the results of the core reports. The optimization of LSTM was chosen by a common algorithm as a conjugate gradient method.

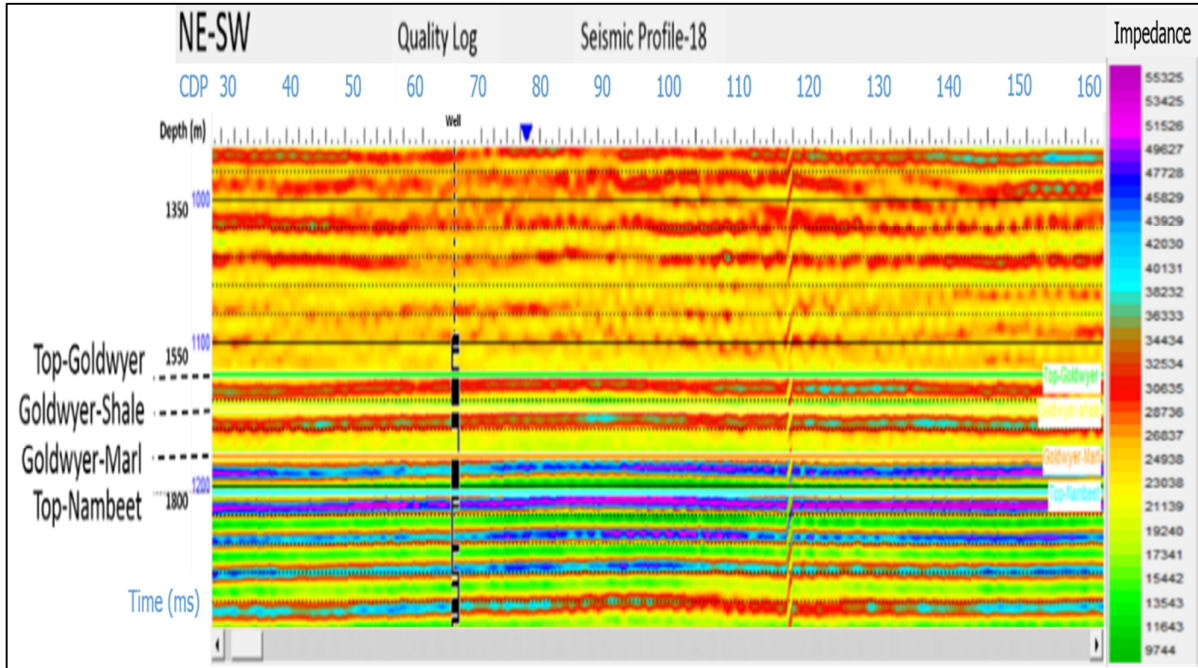


Figure 3. Model-based inverted acoustic impedance in seismic profile 18, where the location of well is shown at CDP 65.

The zoning results show that the facies in this seismic section are divided into two main zones. According to the core reports, the blue parts can be considered as the good quality (GQ) zones, and the green parts can be considered as the bad quality (BQ) zones in the figure. This shows that the complexities in the model are identified using the deep learning algorithm. Of course, it is clear that in some depths, the clustering is not done well and some inter-layers are located between the zones. Nonetheless, these inter-layers do not have much effect on the final interpretation (Figure 4). The accuracy of this method is better evaluated by

extracting an estimated column of zoning quality at the well location of a 2D cross-section (Figure 4) and compared with the actual data (based on the core reports and geochemical data) for this well. Although the proposed method has an accurately modeled two existing zones, the zoning related to the bad quality of gas facies is less accurate (Table 2 and Figure 6). By comparing the real data and the model results at the well location, it can be found that the offered model has an acceptable accuracy. According to the confusion matrix, the suggested zoning accuracy is 86% (Table 2).

Table 1. Specifications of the designed LSTM network.

Type	Value
Input layer	Petrophysical logs & acoustic impedance
Input gate	Sigmoid
Update gate	Sigmoid
Transfer function from input to cell state	Tangent (hyperbolic)
Transfer function from output to cell state	Tangent (hyperbolic)
Output gate	Sigmoid
Initial weight to regularization	0.001
Sparsity regularization	4
Sparsity proportion	0.05
Hidden size	10
Max epochs	50

In order to compare the results of the LSTM network with those of a conventional intelligent

method, a MLP network was designed to apply the same data. The results of zoning by the MLP neural

network can be seen as a 2D zoning section in Figure 5. Its modelling accuracy is also seen in Table 2, which is (78%) less than that (86%) attained by the LSTM network. This indicates a better accuracy of the deep learning method. The noteworthy point in this table is that in addition to the fact that the LSTM network is more accurate than the MLP network, in the LSTM network, the difference in accuracy in determining the two zones is close to each other but this difference in the MLP network is more than the LSTM network. This specifies that the LSTM network is less dependent on the amount of data in the two zones.

The difference in the performance of the two networks in zoning can also be seen in Figure 6.

This figure shows that the LSTM network is better than the MLP network at the well location. It can also be seen in Figure 6 that the designed LSTM network has a good performance for the border detection between these two zones. Nevertheless, at distances farther from the well, some noise can be seen in the seismic section (Figs. 4 and 5). This distortion may be due to the structural factors such as the anisotropy, heterogeneity, low-maturity of organic matter, changes in porosity and shale permeability or estimation errors. Some of them (such as the depth of 1820 m to 1930 m) may be due to the changes in the rock material (shale and marl).

Table 2. Confusion matrix of LSTM network and MLP at the well location.

	LSTM	MLP
<b>Confusion Matrix</b>	$\begin{bmatrix} 91.4 & 8.6 \\ 19.7 & 80.3 \end{bmatrix}$	$\begin{bmatrix} 85.7 & 14.3 \\ 29.9 & 70.1 \end{bmatrix}$
<b>Accuracy of classification (%)</b>	<b>86</b>	<b>78</b>

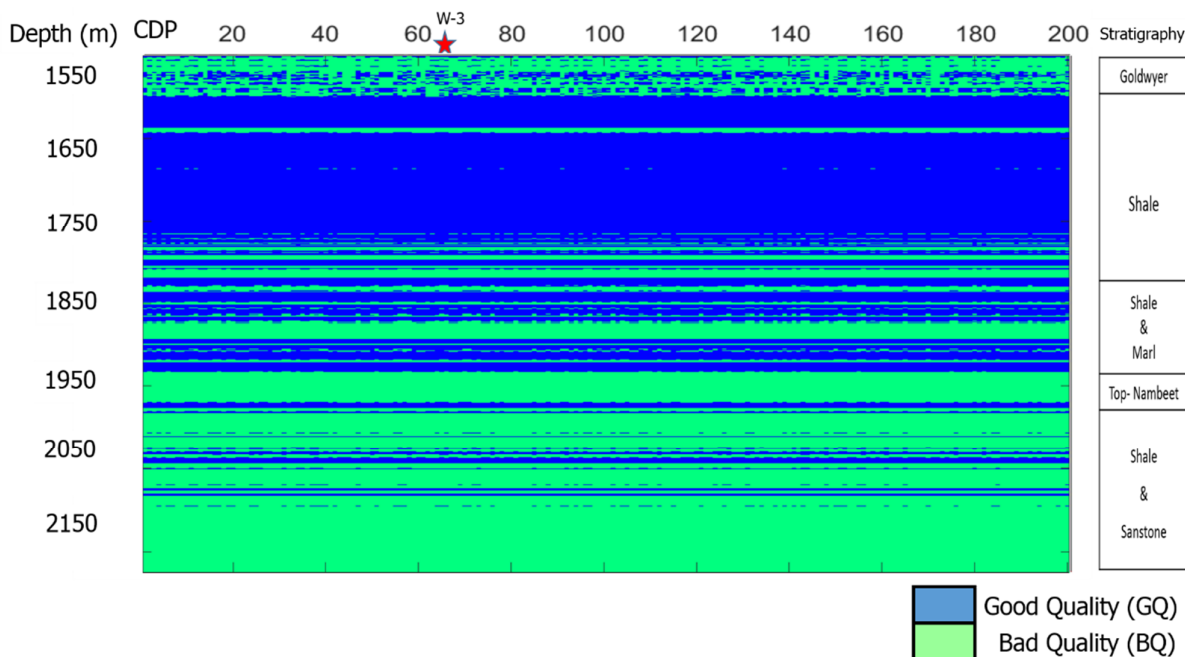


Figure 4. Results of the zoning of facies quality of the designed LSTM network as an unsupervised deep learning technique along seismic profile.

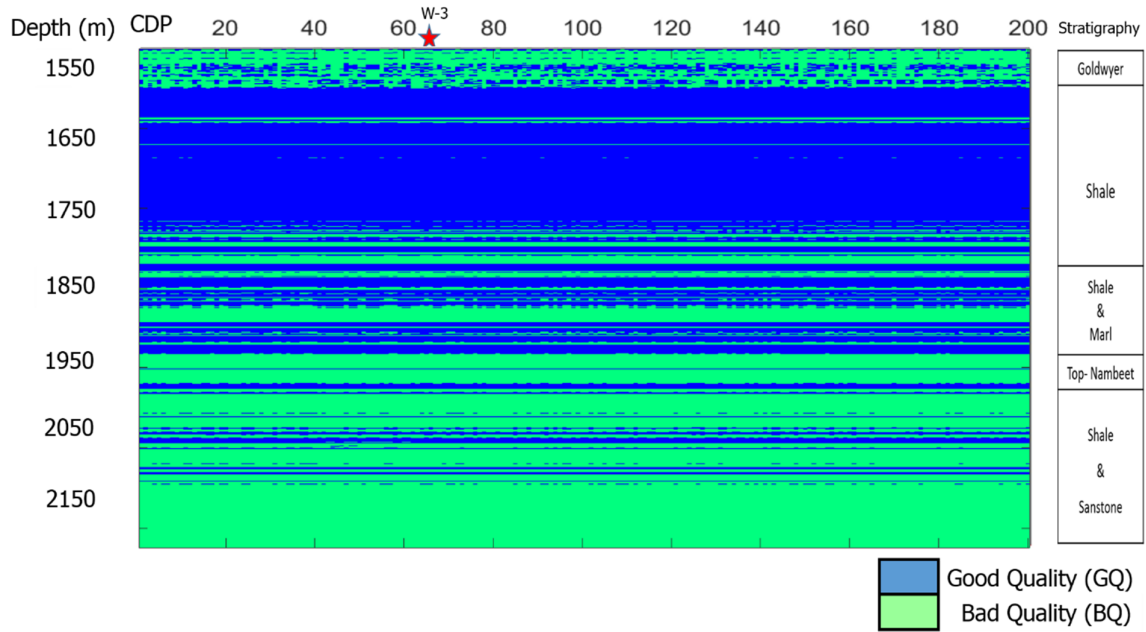


Figure 5. Results of the zoning of facies quality of the designed MLP network as an unsupervised technique along seismic profile.

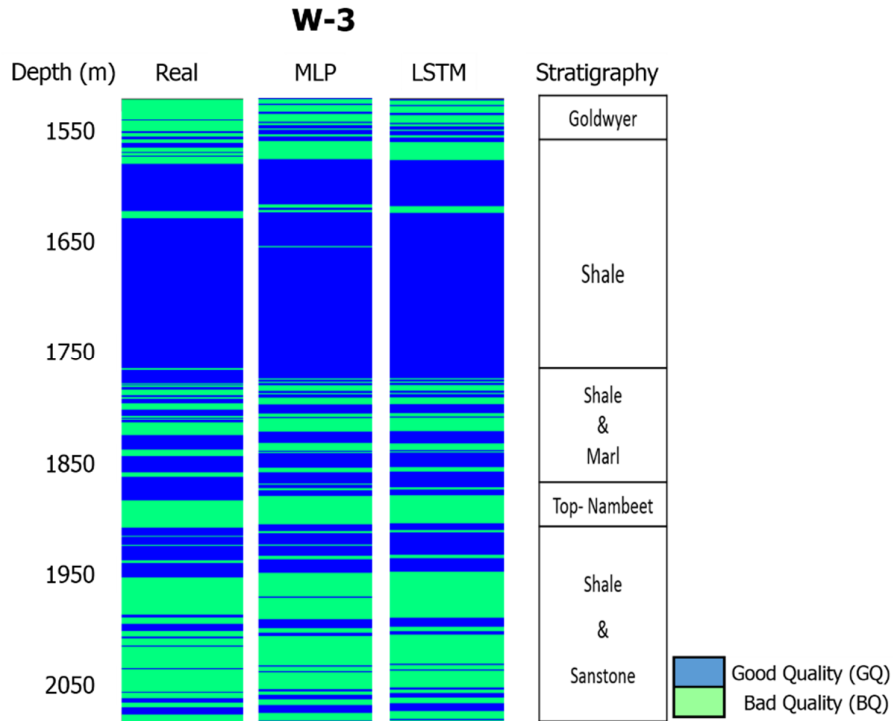


Figure 6. Graphical comparison between the zoning results of real data (left column) and those acquired using MLP (second column) and deep learning technique (third column) at the location of the specified well. The litho-stratigraphy column of the well is in right column.

**5. Conclusions**

This paper proposes a novel approach for zoning the facies quality from well logs and seismic data using an unsupervised deep learning technique; this is an unsupervised LSTM network. The input

data are seven well logs (i.e. GR, DT, CALI, NPFI, RHOB, LLD, and SP) related to a well, and one set of 2D seismic acoustic impedance of the Canning basin. The results obtained show that the quality zoning of gas facies has been done well with an

overall accuracy of 86% using the proposed method. However, its accuracy is reduced at some depth intervals. The zoning accuracy within some inter-layers may be affected by several factors such as the geological, environmental, and structural noise, lack of data labeling, data deficiency, and presence of the immature organic matter. Of course, it is notable that as the distance from the well increases, more noise is seen in the model, which may be due to the lack of the real data at distances farther from the well. Another important advantage of the proposed method is that it does not suffer from over-fitting in zoning, which can be seen in determining these inter-layers. Moreover, unlike the conventional methods in zoning and clustering, the proposed method has a good performance in border detection between the zones. Another major advantage of this method over the conventional intelligent methods such as MLP is that in the deep learning networks, the feature extraction is done automatically. This superiority is clearly seen in the results obtained from this work; the difference in accuracy in determining each zone in the LSTM network was 11.1%, and in the MLP network, it was 15.6%. This advantage is very important in the field of earth sciences, where the data for different classes is usually small and not equal.

### Acknowledgments

The authors would like to appreciate the Department of Mines and Petroleum of WA Government, for their support in providing the data and information.

### References

- [1]. Curtis, J.B., (2002). Fractured shale-gas systems. AAPG Bull. 86 (11), 1921–1938.
- [2]. Clackson, C., Haghshenas, B., Ghanizadeh, A. *et al.*, (2016). Nano pores to mega fractures: current challenges and methods for shale gas reservoir and hydraulic fracture characterization. J. Nat. Gas Sci. Eng. 31, 612–657.
- [3]. Chen, L., Lu, Y.C., Jiang, S., Li, J. Q., Guo, T. L., Luo, C., and Xing, F. C., (2015). Sequence stratigraphy and its application in marine shale gas exploration: A case study of the Lower Silurian Longmaxi Formation in the Jiaoshiba shale gas field and its adjacent area in southeast Sichuan Basin, SW China. Journal of Natural Gas Science and Engineering, 27, 410-423.
- [4]. Ma, Y.Q., Fan, M.J., Lu, Y.C., Guo, X.S., Hu, H.Y., Chen, L., Wang, C., and Liu, X.C., (2016). Geochemistry and sedimentology of the Lower Silurian Longmaxi mudstone in southwestern China: Implications for depositional controls on organic matter accumulation. Marine and Petroleum Geology, 75, 291-309.
- [5]. Jiang, S., Chen, L., Wu, Y., Jiang, Z.L., and McKenna, E., (2017). Hybrid plays of Upper Triassic Chang7 lacustrine source rock interval of Yanchang Formation, Ordos Basin, China. Journal of Petroleum Science and Engineering, 159, 182-196.
- [6]. Shi, M., Yu, B.S., Xue, Z.P., Wu, J.S., and Yuan, Y., (2015). Pore characteristics of organic-rich shales with high thermal maturity: A case study of the Longmaxi gas shale reservoirs from well Yuye-1 in southeastern Chongqing, China. Journal of Natural Gas Science and Engineering, 26, 948-959.
- [7]. Yang, R., He, S., Hu, Q., Hu, D., and Yi, J., (2017). Geochemical characteristics and origin of natural gas from Wufeng-Longmaxi shales of the Fuling gas field, Sichuan Basin (China). International Journal of Coal Geology, 171, 1-11.
- [8]. Doner, Z., Kumral, M., Demirel, I. H., & Hu, Q., (2019). Geochemical characteristics of the Silurian shales from the central Taurides, southern Turkey: Organic matter accumulation, preservation and depositional environment modeling. Marine and Petroleum Geology, 102, 155-175.
- [9]. Cavelan, A., Boussafir, M., Rozenbaum, O., & Laggoun-Défarage, F., (2019). Organic petrography and pore structure characterization of low-mature and gas-mature marine organic-rich mudstones: Insights into porosity controls in gas shale systems. Marine and Petroleum Geology, 103, 331-350.
- [10]. Ying Tang, Runze Yang, Shuai Yin, Tailiang Fan, Lingfeng Dong, and Yunchao Hou., (2019). Analysis of continental shale gas accumulation conditions in a rifted basin: A case study of Lower Cretaceous shale in the southern Songliao Basin, northeastern China. Marine and Petroleum Geology 101. 389–409.
- [11]. Chen, S., Zhao, W., Xinming, G., Zeng, Q., Yang, Q., and Gai, S., (2018) Predicting gas content in high-maturity marine shales using artificial intelligence based seismic multiple-attributes analysis: A case study from the lower Silurian Longmaxi Formation, Sichuan Basin, China, Marine and Petroleum Geology (2018), doi: <https://doi.org/10.1016/j.marpetgeo.2018.11.043>.
- [12]. Passey, Q.R., Creaney, S., Kulla, J.B., Moretti, F.J., and Stroud, J.D. (1990) A practical model for organic richness from porosity and resistivity log. AAPG Bull. 74 (12), 1777e1794.
- [13]. Shuangbiao Han, Jinchuan Zhang, Chao Yang, Songtao Bai, Longxing Huang, Wei Dang, and Chengshan Wang. (2016). Well log evaluation of shale gas reservoirs and preservation conditions of Lower Cambrian shale succession in Cengong Block of southeast Sichuan basin, south China. Journal of Natural Gas Science and Engineering 33. 337e346.

- [14]. Lashin, A. & Mogren, S., (2012). Total organic carbon enrichment and source rock evaluation of the Lower Miocene rocks based on well logs: October oil field, Gulf of Suez-Egypt. *Int J Geosci*, 3, 683-695.
- [15]. Liu, L., Shang, X., Wang, P., Guo, Y., Wang, W., & Wu, L., (2012). Estimation on organic carbon content of source rocks by logging evaluation method as exemplified by those of the 4th and 3rd members of the Shahejie Formation in western sag of the Liaohe Oilfield. *Chinese Journal of Geochemistry*, 31(4), 398-407.
- [16]. Guo, S. & Peng, Y., (2019). "Determination method of shale gas content: A case study in the Ordos Basin, China". *Journal of Petroleum Science and Engineering*, 173, 95-100 .
- [17]. Rui, J., Zhang, H., Zhang, D., Han, F., & Guo, Q., (2019). Total organic carbon content prediction based on support-vector-regression machine with particle swarm optimization. *Journal of Petroleum Science and Engineering*.
- [18]. Rui, J., Zhang, H., Ren, Q., Yan, L., Guo, Q., & Zhang, D., (2020). TOC content prediction based on a combined Gaussian process regression model. *Marine and Petroleum Geology*, 104429.
- [19]. Handhal, A. M., Al-Abadi, A. M., Chafeet, H. E., & Ismail, M.J., (2020). Prediction of total organic carbon at Rumailla oil field, Southern Iraq using conventional well logs and machine learning algorithms. *Marine and Petroleum Geology*, 104347.
- [20]. Zhu, L., Zhang, C., Zhang, C., Zhang, Z., Zhou, X., Liu, W. *et al.*, (2020). A new and reliable dual model-and data-driven TOC prediction concept: A TOC logging evaluation method using multiple overlapping methods integrated with semi-supervised deep learning. *Journal of Petroleum Science and Engineering*, 106944.
- [21]. Altowairqi, Y., Rezaee, R., and Evans, B., (2015). Shale elastic property relationships as a function of total organic carbon content using synthetic samples. *Journal of Petroleum Science & Engineering*. 133,392-400
- [22]. Ashraf, U., Zhu, P., Yasin, Q., Anees, A., Imraz, M., Mangi, H.N., and Shakeel, S., (2019) Classification of reservoir facies using well log and 3D seismic attributes for prospect evaluation and field development: A case study of Sawan gas field, Pakistan, *Journal of Petroleum Science and Engineering*, doi: <https://doi.org/10.1016/j.petrol.2018.12.060>.
- [23]. Chopra, S, Sharma, R., Keay, J., and Marfurt, K., (2012). Shale gas reservoir characterization workflows. *Expanded Abstracts of 82rd Annual International SEG Mtg*. 1-5.
- [24]. Yang, R.Z., Zhao, Z.G., and Pang, H.L., (2012). Shale gas sweet spots: Geological controlling factors and seismic prediction methods. *Earth Science Frontiers*. 19(5), 339-347.
- [25]. Sharma, R. K., Chopra, S., (2015). Identification of thin sweet spots in the Duvernay Formation of north central Alberta. *Seg Technical Program Expanded*.1949, 1802-1806.
- [26]. Daniel J.K., Ross, R., and Marc Bustin., (2009). The importance of shale composition and pore structure upon gas storage potential of shale gas reservoirs. *Marine and Petroleum Geology*. 26(6), 916-927.
- [27]. Kennard, J., Jackson, M., Romine, K., Shaw, R., & Southgate, P., (1994). Depositional sequences and associated petroleum systems of the Canning Basin, WA.
- [28]. Quintavalle, M. & Playford, G. (2008). Stratigraphic distribution of selected acritarchs in the Ordovician subsurface, Canning Basin, Western Australia. *Revue de micropaléontologie*, 51(1), 23-37.
- [29]. Garcia, M. P., Sanchez, G., Dentith, M., & George, A., (2014). Regional structural and stratigraphic study of the Canning Basin, Western Australia: Department of Mines and Petroleum Government of Western Australia.
- [30]. King, M., (1998). The Palaeozoic Play in the South Canning Basin-Results of Looma 1.
- [31]. Romine, K., Southgate, P., Kennard, J., & Jackson, M., (1994). The Ordovician to Silurian phase of the Canning Basin WA: structure and sequence evolution.
- [32]. Brown, S., Boserio, I., Jackson, K., & Spence, K., (1984). The geological evolution of the Canning Basin-implications for petroleum exploration.
- [33]. Geological Survey of Australia and Petroleum and Royalties Division, (2007). Summary of petroleum prospectively, Western Australia 2007: Bonaparte, Bight, Canning, Officer, Perth, Northern Carnarvon, and Southern Carnarvon Basins: Western Australia Geological Survey, 32p.
- [34]. Foster, C.B., O'Brien, G.W., & and Watson, S.T., (1986). Hydrocarbon source potential of the Goldwyer Formation, Barbwire Terrace, Canning Basin, Western Australia. *APEA Journal*, 26, p142-155.
- [35]. Barat, C. & Ducottet, C., (2016). String representations and distances in deep convolutional neural networks for image classification. *Pattern Recognition*, 54, 104-115.
- [36]. Li, Y, Xie, W, and Li, H, (2017) Hyperspectral image reconstruction by deep convolutional neural network for classification, *Pattern Recognition* 63. 371–383.
- [37]. <http://colah.github.io/posts/2015-08-Understanding-LSTMs/>.
- [38]. Nurhaida, I., Noprisson, H., Ayumi, V., Wei, H., Putra, E. D., Utami, M., & Setiawan, H., (2020). Implementation of Deep Learning Predictor (LSTM) Algorithm for Human Mobility Prediction.

## زون‌بندی کیفیت رخساره‌ها در شیل‌های گازی توسط روش یادگیری عمیق

یوسف عسگری نژاد و علی مرادزاد\*

دانشکده مهندسی معدن، پردیس دانشکده‌های فنی، دانشگاه تهران، تهران، ایران

ارسال ۲۰۲۰/۱۲/۱۶، پذیرش ۲۰۲۱/۱/۲۰

\* نویسنده مسئول مکاتبات: a\_moradzadeh@ut.ac.ir

### چکیده:

یکی از مهمترین عواملی که در ذخایر غیر متعارف گاز برای حفاری و تولید نقش دارد، تعیین کیفیت رخساره‌های مناسب است. روش‌های مطالعه مستقیم مغزه و تجزیه و تحلیل ژئوشیمیایی رایج ترین روش‌های مورد استفاده برای مطالعه این کیفیت است. به دلیل کمبود این داده‌ها و هزینه زیاد تولید آن‌ها، محققان اخیراً به روش‌های غیرمستقیم که در آن‌ها از داده‌های متداول مخزن (از جمله نگارهای پتروفیزیکی و داده‌های لرزه‌ای) استفاده می‌شود روی آورده‌اند. یکی از مشکلات عمده در استفاده از این روش‌ها این است که نمی‌توان پیچیدگی‌های این مخازن را به طور دقیق مدل‌سازی کرد. در این مطالعه، کیفیت رخساره‌ها در شیل‌های گازی با استفاده از روش یادگیری عمیق زون‌بندی می‌شود. روش اعمال شده شبکه عصبی حافظه کوتاه مدت بلند (LSTM) است. در این روش، ویژگی‌های مورد نیاز برای زون‌بندی به طور خودکار استخراج شده و برای مدل‌سازی صحیح پیچیدگی‌های مخزن مورد استفاده قرار می‌گیرد. نتایج این کار نشان می‌دهد که زون‌بندی با دقت مناسب (۸۶٪) با استفاده از شبکه عصبی LSTM انجام شده است. در حالی که برای یک شبکه عصبی رایج MLP دقت آن ۷۸٪ است. این امر برتری دقت روش یادگیری عمیق را مشخص می‌کند.

**کلمات کلیدی:** زون‌بندی کیفیت رخساره‌ها، یادگیری عمیق، نگارهای پتروفیزیکی، داده لرزه‌نگاری، حوضه کنینگ.